years ago[11]. Although rhizobia have been studied for more than 100 years, symbionts of less than 10% of the 750 legume genera have been fully characterized. Our work suggests that characterization of the symbionts of the yet unexplored legumes may reveal the rhizobial nature of additional members of the β-Proteobacteria and possibly other taxonomic classes. Such a study may contribute significantly to the understanding of the origin, and the evolution of, the legume–rhizobia symbioses, and may open new perspectives for engineering beneficial associations. □

Methods

Strains and culture conditions

Strain STM678 was provided by H. P. Spaink (Univ. Leiden). Cells were maintained and grown on yeast extract–mannitol medium[2].

DNA amplification, sequencing and analysis

Nearly full-length 16S rDNA was amplified and sequenced as previously described[2]. 16S rDNA PCR-RFLP analysis was performed as described[2] except that *Cfr*13I, *Hinf*I and *Msp*I were used. A 870-bp part of *dnaK* was amplified and sequenced using the primers 5′-GAMGTCAARCGBATCATCAA-3′ and 5′-TGTCYTTVGCBSMNACRTGCAG-3′. A 370-bp fragment of 23S rRNA gene was amplified and sequenced using the universal primers 5′-AGAGGCGATGAAGGACGT-3′ and 5′-ACCTTTCCCTCACGGTACT-3′. A 1,509-bp fragment containing partial *nifH* and *nifD* genes were amplified using the primers 5′-GCCWTCTAYGGNAARGGNGG-3′ and 5′-ATCAGGCCGATCGGGCATT-3′ and further sequenced. A 2.6-kb fragment containing the *nodAB* genes of strain STM678 was amplified using the primers 5′-CAGATCNAGDCCBTTGAARCGCA-3′ (located at the end of *nodD* in rhizobia) and 5′-CTNCGNGCCCARCGNAGTTG-3′ (located within *nodC* in rhizobia). This fragment was further sequenced using pairs of degenerate primers defined from conserved motifs of *nodA*, *nodB*, *nodC*, and *nod* box. Two 1-kb overlapping fragments containing part of the *nodC* and *nodI* genes of strain STM678 were amplified using the primer pairs 5′-TAYRTGGTYGAYGACGGWTC-3′/5′-CCATACGCACCGTGG TGCTCTTGC-3′ and 5′-GGTTATCGGACCGAGTACG/5′-TCTTCCATVAWRTGVGT NGTCA-3′ (forward primer located at the beginning of *nodC* in rhizobia, reverse primer located within *nodI* in rhizobia) and further sequenced. *nodA* PCR-RFLP analysis was performed on a 455-bp PCR product obtained with the primer pair 5′-TCACARCTC KGGCCCGTTCCG-3′/5′-TGGGCSGGNGCNAGRCCBGA-3′ and digested with *Cfr*13I, *Hinf*I and *Hae*III. Multiple alignments were performed with CLUSTALX[12]. Phylogenetic analyses used the neighbour-joining method and the programmes in PAUP version 4.0b5[13].

Construction of a *nodA* mutant

A 2.5-kb *Xho*I-*Xho*I fragment containing the *nodAB* genes of strain STM678 was obtained by PCR amplification using modified primers containing additional *Xho*I sites and cloned in the *Sal*I site of pJQ200mp18 suicide vector[14]. The 4.7-kb *Sal*I *lacZ*-kanamycin-resistance cassette of pKOK5[15] was inserted at the *Sal*I site of the *nodA* gene cloned in pJQ200mp18. The pJQ200 derivatives obtained, which encoded a counterselectable *sacB* marker, were transformed into *Escherichia coli* XLII, and further introduced by conjugation into a spontaneous chloramphenicol-resistant derivative of strain STM678. Transconjugant colonies grown on YM medium containing 50 μg ml^{-1} kanamycin and 100 μg ml^{-1} chloramphenicol were plated onto YM medium containing 7% sucrose and kanamycin. Sucrose-resistant colonies were screened by PCR to ensure replacement of the wild-type *nodA* gene by the *nodA::lacZ* mutated gene. The *Burkholderia* status of the mutated strain was assessed by 16S rDNA PCR-RFLP.

Plant tests

Seeds were surface-sterilized with concentrated sulphuric acid for 5 min. Plant cultivation and nodulation tests were carried out as described[2]. Effectiveness was estimated by visual observation of plant vigour and foliage colour of 30-day-old plants. Sections were made using a Leica VT1000S Vibratome, and examined after staining with 0.01% methylene blue.

Received 22 January; accepted 2 May 2001.

1. Young, J. P. W. & Haukka, K. E. Diversity and phylogeny of rhizobia. *New Phytol.* **133,** 87–94 (1996).
2. Sy, A. *et al.* Methylotrophic *Methylobacterium* nodulate and fix nitrogen in symbiosis with legumes. *J. Bacteriol.* **183,** 214–220 (2001).
3. Lerouge, P. *et al.* Symbiotic host-specificity of *Rhizobium meliloti* is determined by a sulphated and acylated glucosamine oligosaccharide signal. *Nature* **344,** 781–784 (1990).
4. Spaink, H. P. *et al.* A novel highly unsaturated fatty acid moiety of lipo-oligosaccharide signals determines host specificity of Rhizobium. *Nature* **354,** 125–130 (1991).
5. van Berkum, P. & Eartly, B. D. in *The Rhizobiaceae* (eds Spaink, H. P., Kondorosi, A. & Hooykaas, P. J. J.) 1–24 (Kluwer Academic, Dordrecht, 1998).
6. Deschodt, C. C. & Strijdom, B. W. Effective nodulation of *Aspalathus linearis* spp. *linearis* by rhizobia from other *Aspalathus* species. *Phytophylactica* **8,** 103–104 (1976).
7. Dénarié, J., Debellé, F. & Promé, J. C. Rhizobium lipo-chitooligosaccharide nodulation factors: signaling molecules mediating recognition and morphogenesis. *Annu. Rev. Biochem.* **65,** 503–535 (1996).
8. Perret, X., Staehelin, C. & Broughton, W. J. Molecular basis of symbiotic promiscuity. *Microbiol. Mol. Biol. Rev.* **64,** 180–201 (2000).
9. Zhang, X. X. *et al.* The common nodulation genes of *Astragalus sinicus* rhizobia are conserved despite chromosomal diversity. *Appl. Environ. Microbiol.* **66,** 2988–2995 (2000).
10. Boone, C., Olsthoorn, M. M. A., Dakora, F. D., Spaink, H. P. & Thomas-Oates, J. Structural characterisation of lipo-chitin oligosaccharides isolated from *Bradyrhizobium aspalati*, microsymbionts of commercially important South African legumes. *Carbohydr. Res.* **317,** 155–163 (1999).
11. Polhill, R. M., Raven, P. H. & Stirton, C. H. in *Advances in Legume Systematics* Part 1 (eds Polhill, R. M. & Raven, P. H.) 1–26 (Royal Botanic Gardens, Kew, 1981).
12. Thompson, J. D., Gibson, T. J., Plewniak, F., Jeanmougin, F. & Higgins, D. G. The CLUSTALX windows interface: flexible strategies for multiple sequence alignment aided by quality analysis tools. *Nucleic Acids Res.* **25,** 4876–4882 (1997).
13. Swofford, D. L. PAUP. Phylogenetic Analysis Using Parsimony (and other Methods) Version 4 (Sinauer Associates, Sunderland, Massachusetts, 1998).
14. Quandt, J. & Hynes, M. F. Versatile suicide vectors which allow direct selection for gene replacement in Gram-negative bacteria. *Gene* **127,** 15–21 (1993).
15. Kokotek, W. & Lotz, W. Construction of a *lac-Z*-kanamycin-resistance cassette, useful for site-directed mutagenesis and as a promoter probe. *Gene* **84,** 467–471 (1989).

Acknowledgements

We thank H. P. Spaink for providing strain STM678, M. Neyra for providing the 23S rRNA primers, Y. Prin for help in microscopy studies and C. Huttel for sending plant material. We also thank J. Cullimore and J. Batut for comments and suggestions.

Correspondence and requests for materials should be addressed to C.B.-M. (e-mail: Catherine.Boivin@mpl.ird.fr). EMBL accession numbers: AJ302311 to AJ302315, AJ302321, AJ306730.

Spatial awareness is a function of the temporal not the posterior parietal lobe

Hans-Otto Karnath, Susanne Ferber & Marc Himmelbach

Department of Cognitive Neurology, University of Tübingen, Hoppe-Seyler-Strasse 3, 72076 Tübingen, Germany

Our current understanding of spatial behaviour and parietal lobe function is largely based on the belief that spatial neglect in humans (a lack of awareness of space on the side of the body contralateral to a brain injury) is typically associated with lesions of the posterior parietal lobe. However, in monkeys, this disorder is observed after lesions of the superior temporal cortex[1], a puzzling discrepancy between the species. Here we show that, contrary to the widely accepted view, the superior temporal cortex is the neural substrate of spatial neglect in humans, as it is in monkeys. Unlike the monkey brain, spatial awareness in humans is a function largely confined to the right superior temporal cortex, a location topographically reminiscent of that for language on the left[2]. Hence, the decisive phylogenetic transition from monkey to human brain seems to be a restriction of a formerly bilateral function to the right side, rather than a shift from the temporal to the parietal lobe. One may speculate that this lateralization of spatial awareness parallels the emergence of an elaborate representation for language on the left side.

Spatial neglect is a characteristic failure to explore the side of space contralateral to a brain lesion. Patients with this disorder behave as if one side of the surrounding space had ceased to exist. Since the early post-mortem studies, we have believed that, in humans, lesions located predominantly in the posterior parietal lobe are critical for this disorder. Analyses of computerized tomography scans of right-hemispheric stroke patients with neglect found that superimposed lateral projections of these lesions centred on the inferior parietal lobule (IPL)[3,4] and the temporo-parieto-occipital (TPO) junction[4]. More recent studies have confirmed the validity of this conclusion although evidence for additional pathology leading

to spatial neglect outside this region has also been reported[5–8]. However, in monkeys, evidence that spatial neglect is associated with such lesions has been less convincing. Ablation studies revealed no or only minimal spatial neglect[9–13]. These observations raised a controversial discussion on the anatomical and functional homology between human and monkey parietal cortex. In view of this seeming discrepancy, we re-assessed the evidence for involvement of the inferior parietal cortex and TPO junction in human spatial neglect.

Our approach was notably different from previous studies of neglect patients because we focused on patients suffering from 'pure' spatial neglect, that is on patients not having additional primary defects in their visual field. This allowed us to study the neural correlate of pure spatial neglect without a bias to posterior visual regions inducing these latter defects. Forty-nine acute stroke patients with severe spatial neglect but no visual-field defects following circumscribed unilateral right-hemispheric brain lesions, consecutively admitted over a five-year period from a well defined recruitment area, were investigated. In 33 of these patients we found lesions affecting cortical areas, whereas lesions in the other 16 patients were confined to subcortical structures, namely the basal ganglia or the thalamus. Of the patients with cortical lesions, 25 (Table 1) showed no concurrent involvement of the basal ganglia or the thalamus; that is, they showed no involvement of those subcortical nuclei known to induce neglect independent of concomitant cortical damage[3,7,14,15]. The superimposed lesion plots of these 25 subjects were compared with 25 right-brain-damaged (RBD) controls (Fig. 1) who likewise had no visual-field defects and cortical lesions without involvement of the basal ganglia or the thalamus. In clear contrast to controls, the lesion overlap in the neglect patients centred on the superior temporal gyrus (STG: Brodmann areas 22 and 42). Neighbouring structures affected were the ventral postcentral gyrus and the operculum. Interestingly, we found no evidence for a predominant involvement of the IPL[3,4,6,7], the TPO junction[4,7,8], the cingulate cortex[7,8] or the middle temporal gyrus[5] in patients with pure spatial neglect. This pattern did not change when we included the eight patients suffering from cortical lesions but with concurrent involvement of the basal ganglia or the thalamus.

For statistical comparison of IPL with STG involvement, we defined the IPL and STG areas in Talairach space[16] and determined (using MRIcro software[17]) to which percentage the individual lesion affected these two regions of interest (Fig. 1d). Between-group comparisons revealed a highly significant difference for the STG (Mann–Whitney $U = 105$, $P < 0.001$) showing that the area of the STG involved was 6.9 times larger in neglect patients (Fig. 1d). There was no such significant difference for the IPL ($U = 301$, $P = 0.801$). The comparison of relative involvement of the STG and the IPL within each group revealed a 3.7 times larger involvement of the STG in neglect patients (Wilcoxon $Z = -3.51$, $P < 0.001$). In controls, this comparison was not significantly different ($Z = -1.07$, $P = 0.285$). Table 2 in Supplementary Information gives coefficients for the correlation of IPL and STG involvement and the behavioural performance of the patients.

The previous results on lesion location in neglect may have resulted from the inclusion of a significant proportion of patients who suffered not only from spatial neglect but also from additional visual-field defects. Hemianopia was present, for example, in 87% of the patients with spatial neglect studied by Vallar and Perani[3] and in 50% of the patients investigated by Perenin[6]. Hence, it is plausible that in many cases lesions involved posterior visual regions, possibly confounding the interpretation of lesion location relevant to spatial neglect. To test this assumption, we studied 11 acute unilateral right-hemispheric stroke patients suffering from both severe spatial neglect and additional visual-field defects who were consecutively admitted over a 1.5-year period from the same recruitment area as for the groups above. Three of these patients showed concurrent involvement of the basal ganglia or thalamus and were not considered in the present analysis (Table 1). During the same period, we found four patients who suffered from an acute right-hemispheric stroke in the same vascular region as the neglect patients with visual-field defects and likewise exhibited visual-field defects but no spatial neglect (Table 1).

If previous conclusions on lesion location in neglect were confounded by concomitant damage of visual cortical structures, the present comparison should reveal the following: (1) a clear difference in lesion location between those patients with pure neglect and those with both neglect and hemianopia (the latter involving also posterior regions); (2) those areas found as the neural correlate of spatial neglect in patients with pure neglect (Fig. 1) are affected in the patients suffering from both neglect and hemianopia; (3) the centre of lesion overlap in patients with neglect and hemianopia is comparable to that reported in earlier studies (that is, involves the IPL and TPO junction); and (4) the posterior parts of lesion overlap in the patients with neglect and hemianopia also overlap in those patients without neglect but with hemianopia due to a stroke in the territory of the same cerebral artery. Our data were in full accor-

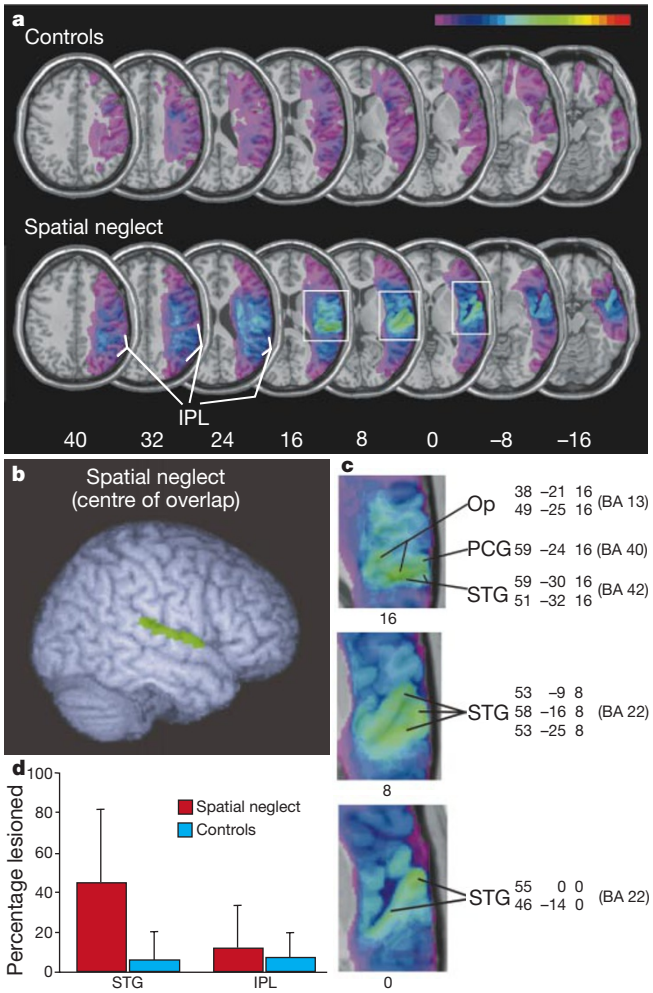

Figure 1 Lesion analysis of patients without (controls) and with spatial neglect. **a**, Overlay plots. Talairach *z*-coordinates[16] of the transverse sections are given. The number of overlapping lesions is illustrated by colour, from violet ($n = 1$) to red ($n = 25$). In line with the criterion used previously[3], the centre of overlap was defined as those voxels that showed lesions in more than 15 patients (green area). IPL, inferior parietal lobule. **b**, **c**, Surface view (**b**) and exploded view (**c**) of the centre of lesion overlap. Talairach coordinates[16] of the locations marked are given. Op, operculum; PCG, ventral postcentral gyrus; STG, superior temporal gyrus; BA, Brodmann area. **d**, Mean percentage of area showing lesions within the STG and within the IPL.

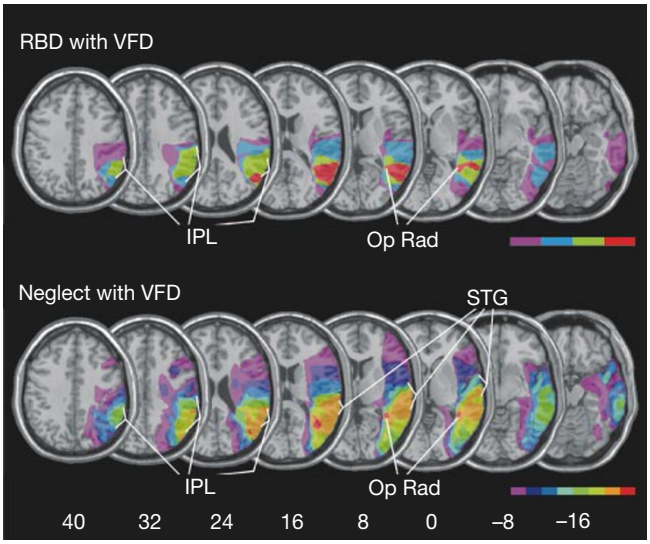

Figure 2 Lesion analysis of patients with visual-field defects (VFDs), without (RBD) and with spatial neglect. Talairach *z*-coordinates[16] of the transverse sections are given. The number of overlapping lesions is illustrated by colour, from violet to red ($n = 1–4$ for RBD, $n = 1–8$ for neglect). The centre of overlap was defined as those voxels that showed lesions in more than 50% of the subjects (green–red area for RBD; green–orange–red area for neglect). IPL, inferior parietal lobule; Op Rad, optic radiation; STG, superior temporal gyrus.

dance with these expectations. The centre of lesion overlap in the patients with both spatial neglect and visual-field defects involved the IPL and the TPO junction, which corresponds to earlier reports[3,4,6–8] (Fig. 2, lower panel). However, the same region was also affected in the patients without neglect but with visual-field defects following a stroke in the territory of the middle cerebral artery (Fig. 2, upper panel). In both groups, visual-field defects were caused by lesion extension to the posterior horn of the lateral ventricle, thereby affecting the optic radiation.

The present finding fits with observations of the consequences of experimental lesions in monkeys. Watson and co-workers[1] found spatial neglect after ablation around both banks of the superior temporal sulcus. Although the focus found here in humans was on the superior temporal gyrus (STG), the observations correspond in that the superior temporal cortex rather than the IPL or the TPO junction is the substrate of spatial neglect in both monkeys and humans. The STG is located at the transition between the two major pathways of cortical visual processing, the 'what' and 'where' systems, respectively[18]. The STG is known to receive polysensory input from both streams thus representing a site of multimodal sensory convergence[19–22]. Our findings indicate that this information may serve as a matrix for spatial exploration and for spatial awareness. The results further indicate that the cytoarchitectonically identical areas 7 in the monkey and in the human are also functionally homologous. In monkeys, lesion of this area in either the right or the left hemisphere causes misreaching for objects with the contralesional arm but not spatial neglect[1,10,11]. The same is true for area-7 lesions in humans[6]. However, unlike area 7 in the parietal cortex, left- and right-hemisphere functions of the STG are different in monkeys and humans. Whereas loss of awareness of the contralesional side in monkeys is observed after lesions of this area in the left or right hemisphere[1,23], spatial neglect in humans is predominantly associated with right-hemispheric lesions[24]. The human superior temporal cortex in the opposite, left hemisphere subserves language functions[2]. Hence, the phylogenetic transition from the monkey to the human brain seems to be a restriction of a formerly bilateral function to the right side, rather than a shift from the temporal to the posterior parietal lobe. One may speculate that this lateralization of spatial awareness parallels the emergence of an elaborate representation of language on the left. However, in contrast to previous conviction, we suggest that parietal lobe organization (probably including human areas 39 and 40 (ref. 25) is in principle comparable and functionally homologous in both species, directly coding space for action. □

Methods

Clinical investigation

Patients were classified as having spatial neglect when they showed the typical clinical behaviour such as spontaneous deviation of the head and eyes toward the ipsilesional side, orienting towards the ipsilesional side when addressed from the front or the left, and ignoring contralesionally located people or objects. In addition, all patients were further assessed with the following four clinical neglect tests and had to fulfil the criterion in at least two of them.

Letter cancellation test[26]: sixty target letters were distributed amid distractors on a horizontally oriented 21 × 29.7 cm sheet of paper, 30 within each half field. Patients had to cancel all target letters and were classified as suffering from spatial neglect when they omitted at least five left-sided targets. Bells test[27]: this consists of seven columns each containing five targets (bells) among distractors. Three of the seven columns (15 targets) are on the left side of a horizontally oriented 21 × 29.7 cm sheet of paper. More than five

Table 1 Demographic and clinical data of patients with spatial neglect and without (controls, RBD)

			Spatial neglect	Controls	Spatial neglect	RBD
			No visual-field defects		With visual-field defects	
Number			25	25	8	4
Sex			14 f, 11 m	11 f, 14 m	5 f, 3 m	1 f, 3 m
Age (yr)		Median (range)	68 (31–89)	63 (33–77)	71 (55–83)	63 (60–79)
Aetiology			20 infarct	21 infarct	7 infarct	3 infarct
			5 haemorrhage	4 haemorrhage	1 haemorrhage	1 haemorrhage
Time since lesion (d)		Median (range)	9 (1–140)	3.5 (1–54)	8 (3–157)	7 (3–22)
Paresis of contralesional side*			100	84	88	50
% present	Arm	Median (range)	2 (0–4.5)	3.5 (0–5)	2.5 (0–5)	3.3 (1.5–5)
	Leg	Median (range)	4 (0–5)	5 (2–5)	4.5 (0–5)	4.8 (4.5–5)
Somatosensory deficit of contralesional	Arm		64	36	88	50
side (touch) (% present)	Leg		64	28	75	50
Visual-field defect (% present)			0	0	100 (7 Ha, 1 Qa)	100 (2 Ha, 2 Qa)
Letter cancellation	Left	Median (range)	1 (0–29)	29 (16–30)	0 (0–21)	29.5 (29–30)
	Right	Median (range)	22 (4–30)	30 (17–30)	18 (11–26)	30 (28–30)
Bells test	Left	Median (range)	0 (0–14)	14 (8–15)	0 (0–11)	15 (14–15)
	Right	Median (range)	11 (2–15)	15 (7–15)	7 (4–14)	15 (14–15)
Baking tray task	Left	Median (range)	4.5 (0–9)	8 (6–10)	2.5 (0–6)	8†
	Right	Median (range)	11 (7–16)	8 (6–10)	13.5 (10–16)	8†
Copying (% omitted)		Median (range)	50 (0–88)	0 (0–25)	75 (38–88)	0†

RBD, right brain damage; f, female; m, male; Ha, hemianopia; Qa, quadrantanopia.
* Paresis was scored with the usual clinical ordinal scale: 0, no trace of movement; to 5, normal movement.
† No variation in data.

left-sided omissions indicated spatial neglect. Baking tray task[28]: patients had to place 16 identical items as evenly as possible on a blank test sheet (21 × 29.7 cm). Any distribution that is more skewed than seven items in the left half and nine on the right[28] was considered a sign of neglect. Copying task: patients were asked to copy a complex multi-object scene consisting of four figures on a 21 × 29.7 cm sheet of paper. Omission of at least one of the left-sided features of each figure was scored as one and omission of each whole figure was scored as two. One additional point was given when left-sided figures were drawn on the right side. The maximum score was eight. A score higher than one, that is, more than 12.5% omissions, indicated neglect.

All other relevant demographic and clinical parameters are shown in Table 1, together with an overview of these data. Visual-field defects were measured by Tübingen perimetry and standardized neurological examination.

Lesion analysis

Brain lesions were identified by computerized tomography or magnetic resonance imaging (MRI). Patients with diffuse or bilateral brain lesions, patients with tumours and patients in whom imaging revealed no manifest lesion were excluded. Lesions were mapped with MRIcro software[17] (http://www.psychology.nottingham.ac.uk/staff/cr1/mricro.html). They were drawn manually on slices of a template MRI scan from the Montreal Neurological Institute (http://www.bic.mni.mcgill.ca/cgi/icbm_view), which is based on 27 T1-weighted MRI scans, normalized to Talairach space[16]. This scan was distributed with SPM99 (http://www.fil.ion.bpmf.ac.uk/spm/spm99.html). For superimposing of the individual brain lesions, the same MRIcro software[17] was used. Three-dimensional rendering was carried out with mri3dX software (http://mrrc11.mrrc.liv. ac.uk/mri3dX).

Received 23 January; accepted 25 April 2001.

1. Watson, R. T., Valenstein, E., Day, A. & Heilman, K. M. Posterior neocortical systems subserving awareness and neglect. *Arch. Neurol.* **51,** 1014–1021 (1994).
2. Binder, J. The new neuroanatomy of speech perception. *Brain* **123,** 2371–2372 (2000).
3. Vallar, G. & Perani, D. The anatomy of unilateral neglect after right-hemisphere stroke lesions. A clinical/CT-scan correlation study in man. *Neuropsychologia* **24,** 609–622 (1986).
4. Heilman, K. M., Watson, R. T., Valenstein, E. & Damasio, A. R. in *Localization in Neuropsychology* (ed. Kertesz, A.) 471–492 (Academic, New York, 1983).
5. Samuelsson, H., Jensen, C., Ekholm, S., Naver, H. & Blomstrand, C. Anatomical and neurological correlates of acute and chronic visuospatial neglect following right hemisphere stroke. *Cortex* **33,** 271–285 (1997).
6. Perenin, M. T. in *Parietal Lobe Contributions to Orientation in 3D Space* (eds Thier, P. & Karnath, H.-O.) 289–308 (Springer, Heidelberg, 1997).
7. Leibovitch, F. S. *et al.* Brain–behavior correlations in hemispatial neglect using CT and SPECT: the Sunnybrook Stroke Study. *Neurology* **50,** 901–908 (1998).
8. Leibovitch, F. S. *et al.* Brain SPECT imaging and left hemispatial neglect covaried using partial least squares: the Sunnybrook Stroke Study. *Hum. Brain Mapp.* **7,** 244–253 (1999).
9. Ettlinger, G. & Kalsbeck, J. E. Changes in tactile discrimination and in visual reaching after successive and simultaneous bilateral posterior parietal ablations in the monkey. *J. Neurol. Neurosurg. Psychiatry* **25,** 256–268 (1962).
10. Lamotte, R. H. & Acuna, C. Deficits in accuracy of reaching after removal of posterior parietal cortex in monkeys. *Brain Res.* **139,** 309–326 (1978).
11. Faugier-Grimaud, S., Frenois, C. & Stein, D. G. Effects of posterior parietal lesions on visually guided behavior in monkeys. *Neuropsychologia* **16,** 151–168 (1978).
12. Lynch, J. C. & McLaren, J. W. Deficits of visual attention and saccadic eye movments after lesions of parietooccipital cortex in monkeys. *J. Neurophysiol.* **61,** 74–90 (1989).
13. Gaffan, D. & Hornak, J. Visual neglect in the monkey. Representation and disconnection. *Brain* **120,** 1647–1657 (1997).
14. Damasio, A. R., Damasio, H. & Chui, H. C. Neglect following damage to frontal lobe or basal ganglia. *Neuropsychologia* **18,** 123–132 (1980).
15. Motomura, N. *et al.* Unilateral spatial neglect due to hemorrhage in the thalamic region. *Acta Neurol. Scand.* **74,** 190–194 (1986).
16. Talairach, J. & Tournoux, P. *Co-planar Stereotaxic Atlas of the Human Brain: 3-Dimensional Proportional System—an Approach to Cerebral Imaging.* (Thieme, New York, 1988).
17. Rorden, C. & Brett, M. Stereotaxic display of brain lesions. *Behav. Neurol.* (in the press).
18. Ungerleider, L. G. & Mishkin, M. in *Analysis of Visual Behavior* (eds Ingle, D. J., Goodale, M. A. & Mansfield, R. J. W.) 549–586 (MIT Press, Cambridge, Massachusetts, 1982).
19. Jones, E. G. & Powell, T. P. S. An anatomical study of converging sensory pathways within the cerebral cortex of the monkey. *Brain* **93,** 793–820 (1970).
20. Seltzer, B. & Pandya, D. N. Afferent cortical connections and architectonics of the superior temporal sulcus and surrounding cortex in the rhesus monkey. *Brain Res.* **149,** 1–24 (1978).
21. Bruce, C., Desimone, R. & Gross, C. G. Visual properties of neurons in a polysensory area in superior temporal sulcus of the macaque. *J. Neurophysiol.* **46,** 369–384 (1981).
22. Felleman, D. J. & Van Essen, D. C. Distributed hierarchical processing in the primate cerebral cortex. *Cereb. Cortex* **1,** 1–47 (1991).
23. Luh, K. E., Butter, C. M. & Buchtel, H. A. Impairments in orienting to visual stimuli in monkeys following unilateral lesions of the superior sulcal polysensory cortex. *Neuropsychologia* **24,** 461–470 (1986).
24. Mesulam, M.-M. Spatial attention and neglect: parietal, frontal and cingulate contributions to the mental representation and attentional targeting of salient extrapersonal events. *Phil. Trans. R. Soc. Lond. B* **354,** 1325–1346 (1999).
25. Darling, W. G., Rizzo, M. & Butler, A. J. Disordered sensorimotor transformations for reaching following posterior cortical lesions. *Neuropsychologia* **39,** 237–254 (2001).
26. Weintraub, S. & Mesulam, M.-M. in *Principles of Behavioral Neurology* (ed. Mesulam, M.-M.) 71–123 (Davis, Philadelphia, 1985).
27. Gauthier, L., Dehaut, F. & Joanette, Y. The bells test: a quantitative and qualitative test for visual neglect. *Int. J. Clin. Neuropsychol.* **11,** 49–54 (1989).
28. Tham, K. & Tegnér, R. The baking tray task: a test of spatial neglect. *Neuropsychol. Rehab.* **6,** 19–25 (1996).

Supplementary information is available on *Nature*'s World-Wide Web site (http://www.nature.com) or as paper copy from the London editorial office of *Nature*.

Acknowledgements

This work was supported by grants from the Deutsche Forschungsgemeinschaft and the Bundesministerium für Bildung, Wissenschaft, Forschung und Technologie awarded to H.-O.K. We thank M. Niemeier, L. Johannsen and U. Zimmer for support with the neuropsychological testing of the patients; P. Thier for discussion and suggestions for the manuscript; U. Amann for help in the tomography archives; and C. Rorden for developing the MRIcro software.

Correspondence and requests for materials should be addressed to H.-O.K. (e-mail: karnath@uni-tuebingen.de).

Single neurons in prefrontal cortex encode abstract rules

Jonathan D. Wallis, Kathleen C. Anderson & Earl K. Miller

Center for Learning and Memory, RIKEN-MIT Neuroscience Research Center, and Department of Brain and Cognitive Sciences, Massachusetts Institute of Technology, Cambridge, Massachusetts 02139, USA

The ability to abstract principles or rules from direct experience allows behaviour to extend beyond specific circumstances to general situations. For example, we learn the 'rules' for restaurant dining from specific experiences and can then apply them in new restaurants. The use of such rules is thought to depend on the prefrontal cortex (PFC) because its damage often results in difficulty in following rules[1]. Here we explore its neural basis by recording from single neurons in the PFC of monkeys trained to use two abstract rules. They were required to indicate whether two successively presented pictures were the same or different depending on which rule was currently in effect. The monkeys performed this task with new pictures, thus showing that they had learned two general principles that could be applied to stimuli that they had not yet experienced. The most prevalent neuronal activity observed in the PFC reflected the coding of these abstract rules.

Neurons in the prefrontal cortex (PFC) encode many different types of information from all stages of the perception–action cycle[2]. They are activated by stimuli from all sensory modalities[3–5], before and during a variety of actions[6–8], during memory for past events[9], in anticipation of expected events and behavioural consequences[10–12], and are modulated by 'internal' factors such as motivational and attentional state[13,14]. The PFC is thought to use this diverse information for the 'higher order' control of behaviour, in particular the application of behaviour-guiding rules that are lost after damage to the PFC[15,16]. Although rules can be specific and concrete (for example, 'red' means 'stop'), it is the abstraction of general rules or principles (those not tied to any particular stimulus or behavioural response) that allows for the flexibility and adaptability that are central to intelligent behaviour. Although recent studies indicate that PFC neurons can encode concrete rules between specific stimuli and behavioural responses[17–19], we do not know how, or even whether, PFC neurons can encode abstract rules.

Thus, we trained two monkeys to switch flexibly between two abstract rules. The 'match' rule required monkeys to release a lever if two successively presented (sample and test) objects were identical, whereas the 'nonmatch' rule required the lever release if the two objects were different (Fig. 1). The rule applicable for each trial was randomly indicated by a cue that was presented with the sample. To separate the neural activity related to the physical properties of the